

# The BU72- $\mu$ opioid receptor crystal structure is a covalent adduct

Thomas A. Munro

*School of Life and Environmental Sciences, Deakin University, Melbourne, Australia*

[t.munro@deakin.edu.au](mailto:t.munro@deakin.edu.au)

[orcid.org/0000-0002-3366-7149](https://orcid.org/0000-0002-3366-7149)

In the crystal structure of BU72 bound to the  $\mu$  opioid receptor, the opioid clashes with an adjacent residue, and unexplained electron density connects the two<sup>1</sup>. It has been reported that this density can be filled by a magnesium ion<sup>2</sup>. However, this proposal requires unrealistically short bonds and an incomplete coordination shell. Moreover, the crystals were prepared without magnesium salts, but with components that can generate reactive oxygen species: HEPES buffer, nickel ions, and an N-terminus that forms redox-active nickel complexes. Here I show that an oxygen atom fills the unexplained density, giving a known type of covalent adduct with reasonable geometry and no clashes. Strain is evident, but is consistent with tension from the tethered N-terminus.

---

As noted in the original report, the truncated N-terminus of the receptor unexpectedly intrudes into the binding pocket. The third residue of the terminus, His54, clashes with the secondary amine of BU72 (Figure 1a). The original PDB validation report gives an N $\cdots$ N overlap of 0.56 Å, excluding hydrogen atoms; adding these would exacerbate the clash. The region of overlap is also filled with unexplained electron density (up to 6.8 $\sigma$ ). This is centered on a point very close to both N atoms ( $\sim$ 1.6 Å). The recent revision of the stereochemistry of BU72 did not resolve these problems<sup>3,4</sup>.

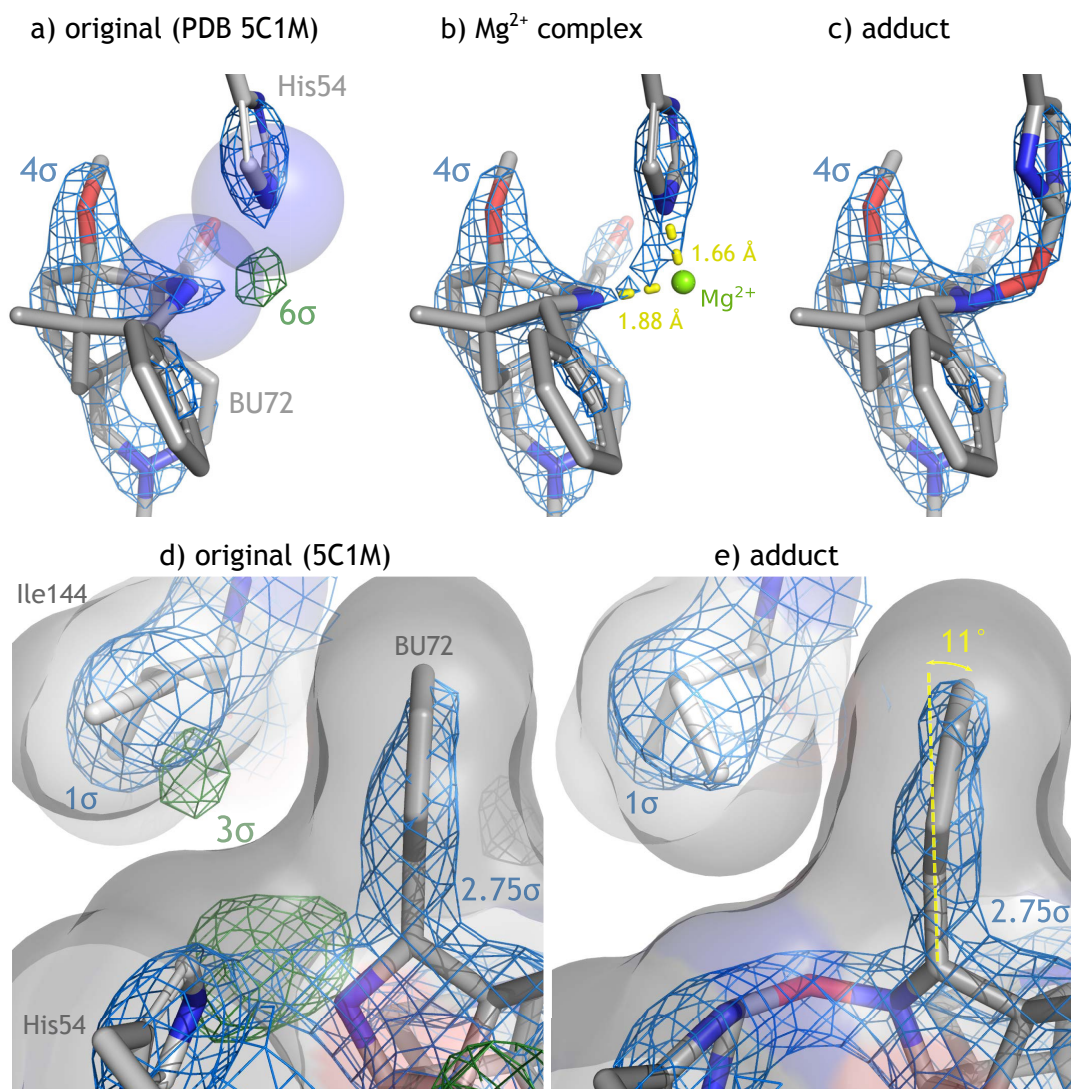


**Figure 1. Comparative fit of models to electron density.**  $2F_o-F_c$  isomesh (blue) and  $F_o-F_c$  omit isomesh (unexplained density in green) are shown at the indicated levels. Clashing N atoms are shown as spheres in (a), and solvent-accessible surfaces in (d) and (e).

It has since been reported that the unexplained density can be filled by a coordinated magnesium ion<sup>2</sup>. This particular metal was reportedly optimal; lithium failed to fill the density, while sodium, nickel, and zinc gave an excess. I confirmed that  $Mg^{2+}$  gave an excellent fit, with no excess or unexplained density above  $2.5\sigma$  (Figure 1b; see Supplementary Information for methods). However, the resulting  $N\cdots Mg$  distances were unrealistic (1.88 and 1.66 Å). Compared

with values from structures of subatomic resolution ( $2.19 \pm 0.06 \text{ \AA}$ , mean  $\pm \sigma$ )<sup>5</sup>, these distances can be confidently rejected, with probabilities of  $<10^{-6}$  and  $<10^{-18}$ , respectively. Note that  $\text{Mg}^{2+}$  is not centered in the density even with these unrealistically short distances, suggesting that the actual bonds are even shorter (Figure 1b). Furthermore, the ion's coordination shell is incomplete, with a coordination number of two rather than the expected four to six<sup>6</sup>. Finally, no source of magnesium was used in the purification and crystallization of the ligand-receptor complex<sup>1</sup>. Collectively, this evidence makes this proposal untenable.

The only metal present in the buffers, sodium, gave a worse fit<sup>2</sup>, and can also be excluded due to even longer  $\text{N}\cdots\text{Na}$  distances ( $2.46 \pm 0.02 \text{ \AA}$ )<sup>5</sup>. Nickel was used for affinity chromatography, and  $\text{N}\cdots\text{Ni}$  distances can be shorter ( $1.88 \pm 0.03 \text{ \AA}$ ). However, as noted above, nickel fitted very poorly, with substantial excess electron density<sup>2</sup>; further evidence against nickel and other heavy metals is the lack of anomalous scattering noted in the original report<sup>1</sup>. Indeed, no metal forms coordination bonds to N of  $<1.76 \text{ \AA}$ .<sup>5</sup> These distances are also much too short to represent non-covalent interactions ( $\geq 2.4 \text{ \AA}$ )<sup>7</sup>, which would also not give rise to the uninterrupted electron density seen connecting the N atoms here (Figures 1d and 1e).

Having excluded metal coordination complexes and non-covalent interactions, the unexplained density appears to represent two covalent bonds from the N atoms to a non-metal approximately isoelectronic with  $\text{Mg}^{2+}$ , such as oxygen. Consistent with this possibility, the experimental conditions used can generate reactive oxygen species. The buffers used for receptor purification and crystallization contained HEPES, which generates hydrogen peroxide on exposure to light<sup>8</sup>. Additionally, the truncated N-terminus Gly-Ser-His, like other Gly-X-His N-termini<sup>9</sup>, forms nickel coordination complexes. Specifically, Gly-Ser-His can capture nickel ions from affinity columns (e.g. PDB [1JVN](#))<sup>10</sup>, which were used for purification of the receptor in this case. The resulting complexes catalyze the decomposition of hydrogen peroxide to reactive oxygen

species<sup>9</sup>. These in turn can oxidize secondary amines<sup>11</sup> and histidine<sup>12</sup>, which contact the unexplained density in this case. Finally, the resulting radicals can be quenched by adduct formation<sup>12</sup>.

Related adducts reported recently (e.g. Figure 2a)<sup>12,13</sup> suggested a potential structure for an oxygen-bridged adduct (Figure 2b). Potential intermediates (N-oxyl and histidyl radicals) are also shown, but are necessarily speculative. The proposed adduct was fitted to the binding site and refined (see Supplementary Information for methods). The adduct gave an excellent fit, with no excess or unexplained density even at  $2\sigma$  (Figure 1c). Both bonds to the oxygen atom were resolved at  $4.2\sigma$  – higher than much of the ligand itself and surrounding side-chains. The lengths of the bonds exclude the possibility that one of them represents a non-covalent interaction, as discussed above. The oxygen atom was well-centered in the density, unlike  $\text{Mg}^{2+}$ .

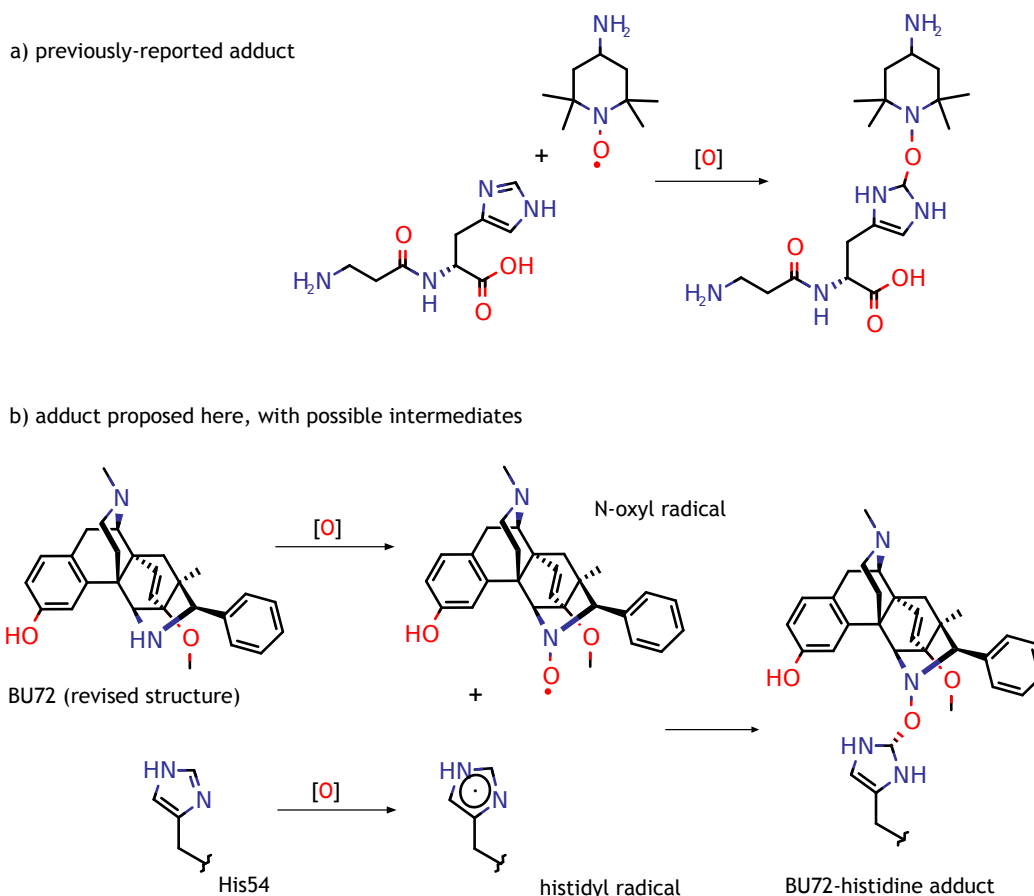


**Figure 2. Chemical structures: a) a recently reported adduct<sup>12</sup>. b) The adduct proposed here, with possible intermediates.**

The geometry of the adduct exhibited more outliers than the revised structure of BU72 fitted in isolation, but fewer than the original structure, and gave acceptable metrics (Table 1). The only severe outlier was the bond angle at the bridging oxygen atom ( $131^\circ$  vs the ideal  $109^\circ$ ;  $Z = 7.2$ ). There are several indications that this is real strain rather than a fitting artefact, however. The angle is clearly resolved at high density, and is consistent with tension from the tethered N-terminus. The same tension is suggested by the phenyl group, which is bent out-of-plane, as if being pulled against Ile144 (Figure 1e); this bend is well-resolved at  $2.75\sigma$ . Furthermore, strain is evident in the N-terminus itself: in both this model and the original, Thr60 exhibits a rare and high-energy *cis*-peptide bond.

	<i>original</i>	<i>revised</i>	
<i>Structure</i>	<b>BU72</b>	<b>BU72</b>	<b>Adduct</b>
<i>Non-hydrogen atoms</i>	32	32	44
<i>Geometric outliers (<math> Z  &gt; 2</math>)</i>	26	0	10
<i>Severe outliers (<math> Z  &gt; 5</math>)</i>	9	0	1
<i>Bond angle RMSZ</i>	3.23	0.66	1.52
<i>Bond length RMSZ</i>	3.32	0.38	1.13
<i>Real-space correlation coefficient (RSCC)*</i>	0.914	0.953	0.951
<i>Real-space R (RSR)</i>	0.090	0.088	0.081

**Table 1. Geometry relative to GRADE restraints, and fit to electron density from PDB validation.** Lower values are better except for RSCC (\*).

A search for alternative ligands in the original study was unsuccessful. The mass spectrum of the crystallization mixture revealed a molecular ion consistent with BU72, but no others of comparable mass<sup>1</sup>. However, the intact adduct would not be detectable in solution, and one decomposition product per binding site would yield negligible concentrations relative to saturating BU72. An alternative test would be for modification of His54: proteolysis of the receptor and mass spectrometry of the fragments should reveal either the adduct or a decomposition product<sup>12</sup>. Adducts of this kind tend to be unstable in the presence of reactive oxygen species. The previous adducts mentioned above were not isolated, but detected only by mass spectrometry<sup>12,13</sup>. However, in this case adduct formation would liberate the nickel ion, ending the catalytic cycle. This may prevent further reaction.

In conclusion, the observed density and distances are not consistent with a coordination complex or noncovalent interactions, and instead appear to represent covalent bonds to a nonmetallic atom approximately isoelectronic

with  $\text{Mg}^{2+}$ . The density firmly establishes the presence of this atom, of the two covalent bonds, and their approximate length and geometry. Oxygen fits all these criteria. The presence of conditions known to give reactive oxygen species, along with prior reports of oxidative adducts of this kind, provide a plausible mechanism. This hypothesis also provides a simple explanation for a puzzling result in the original report: despite the extremely strong interaction implied by the structure itself, removal of the side chain of His54 by mutagenesis had no detectable effect on the affinity or potency of BU72<sup>1</sup>. Since the full-length receptor used in those binding assays lacks the Gly-Ser-His N-terminus, the mechanism proposed here could not occur, and thus binding would be unaffected by the presence or absence of His54.

**Acknowledgment:** Robbie Joosten kindly modified the code of PDB-REDO server to enable refinement of the adduct.

**Supporting Information available:** Methods; coordinates (mmCif), reflections (MTZ), and PDB validation reports (PDF and xml) for the  $\text{Mg}^{2+}$  complex and the BU72- $\mu\text{OR}$  adduct; ideal structure (pdb) and restraints (mmCif) for the BU72-histidine adduct; ligand distortions and Z scores (xlsx); molecular structures (cml). An interactive side-by-side visualization of the adduct and original model is available at: <https://molstack.bioreproducibility.org/p/Y7FU>

## Bibliography

- 1 Huang, W. *et al.* Structural insights into  $\mu$ -opioid receptor activation. *Nature* **524**, 315–321 [doi.org/f7m78z](https://doi.org/10.1038/f7m78z) (2015).
- 2 Chan, H. C. S. *et al.* Enhancing the signaling of GPCRs via orthosteric ions. *ACS Central Science* **6**, 274–282 [doi.org/dk25](https://doi.org/10.1021/dk25) (2020).
- 3 Munro, T. A. Revised ( $\beta$ -phenyl) stereochemistry of ultrapotent  $\mu$  opioid BU72. *bioRxiv* [doi.org/dq7s](https://doi.org/10.1101/dq7s) (2020).
- 4 Huang, W. *et al.* Author Correction: Structural insights into  $\mu$ -opioid receptor activation. *Nature* **584**, E16 [doi.org/d5jj](https://doi.org/10.1038/d5jj) (2020).
- 5 Kuppuraj, G., Dudev, M. & Lim, C. Factors governing metal–ligand distances and coordination geometries of metal complexes. *Journal of Physical Chemistry B* **113**, 2952–2960 [doi.org/dqgnpj](https://doi.org/10.1021/dqgnpj) (2009).
- 6 Dudev, M., Wang, J., Dudev, T. & Lim, C. Factors governing the metal coordination number in metal complexes from Cambridge Structural Database analyses. *Journal of Physical Chemistry B* **110**, 1889–1895 [doi.org/dbw84h](https://doi.org/10.1021/dbw84h) (2006).
- 7 Kruse, H., Sponer, J. & Auffinger, P. Comment on “Evaluating unexpectedly short non-covalent distances in X-ray crystal structures of proteins with electronic structure analysis”. *Journal of Chemical Information and Modeling* **59**, 3605–3608 [doi.org/d8jz](https://doi.org/10.1021/d8jz) (2019).
- 8 Masson, J.-F., Gauda, E., Mizaikoff, B. & Kranz, C. The interference of HEPES buffer during amperometric detection of ATP in clinical applications. *Analytical and Bioanalytical Chemistry* **390**, 2067–2071 [doi.org/fhkf72](https://doi.org/10.1007/s00216-008-1722-2) (2008).
- 9 Ueda, J.-i., Ozawa, T., Miyazaki, M. & Fujiwara, Y. SOD-like activity of complexes of nickel(II) ion with some biologically important peptides and their novel reactions with hydrogen peroxide. *Inorganica Chimica Acta* **214**, 29–32 [doi.org/d8dbw9](https://doi.org/10.1016/0162-0134(93)80009-9) (1993).
- 10 Chaudhuri, B. N. *et al.* Crystal structure of imidazole glycerol phosphate synthase: a tunnel through a ( $\beta/\alpha$ )<sub>8</sub> barrel joins two active sites. *Structure* **9**, 987–997 [doi.org/cjmk4z](https://doi.org/10.1016/S0969-2126(01)00441-1) (2001).
- 11 Aurich, H. G. Nitroxides. *Patai's Chemistry of Functional Groups*, 313–370 [doi.org/cp3635](https://doi.org/10.1016/S0360-3917(08)00363-5) (1989).
- 12 Ihara, H. *et al.* 2-Oxo-histidine-containing dipeptides are functional oxidation products. *Journal of Biological Chemistry* **294**, 1279–1289 [doi.org/d7n6](https://doi.org/10.1074/jbc.M109.047166) (2019). See figure 7c.
- 13 Chen, J.-H. *et al.* TEMPO-mediated synthesis of *N*-(fluoroalkyl)imidazolones via reaction of imidazoles with iodofluoroacetate. *Advanced Synthesis & Catalysis* **362**, 269–276 [doi.org/d7v3](https://doi.org/10.1002/adsc.202000032) (2020). See compound **32**.